Table 1. The operating points estimated from equilibrium diagram

	Supine	Upright tilt	Simulated upright tilt without resetting of the neural arc
AP (mmHg)	102 ± 4	102 ± 4	92 ± 3*†
SNA (a.u)	66 ± 6	91 ± 5*	79 ± 5*†

Values are means ± S.D. ($n = 8$). *$P < 0.05$ *versus* Supine. †$P < 0.05$ Upright tilt *versus* Simulated upright tilt without resetting of the neural arc.

Table 2. Effect of upright tilt on the baroreflex neural and peripheral arc parameters

	Supine	Upright tilt
Neural arc		
P_1 (a.u.)	94 ± 2	112 ± 5*
P_2 (a.u. mmHg^{-1})	0.10 ± 0.01	0.09 ± 0.02
P_3 (mmHg)	109 ± 6	109 ± 6
P_4 (a.u.)	4 ± 1	29 ± 6*
G_{max} (a.u. mmHg^{-1})	−2.5 ± 0.4	−2.3 ± 0.4
Peripheral arc		
P_1 (mmHg)	115 ± 18	82 ± 12*
P_2 (mmHg a.u.$^{-1}$)	−0.04 ± 0.01	−0.05 ± 0.01
P_3 (a.u.)	63 ± 8	88 ± 7*
P_4 (mmHg)	50 ± 9	50 ± 5
G_{max} (mmHg a.u.$^{-1}$)	1.2 ± 0.4	1.0 ± 0.1

Values are means ± S.D. ($n = 8$). See eqn (1) in Methods for definition of the four parameters of the logistic function. *$P < 0.05$, Supine *versus* Upright tilt.

Table 3. Effect of upright tilt on the baroreflex total arc parameters

	Supine	Upright tilt
P_1 (mmHg)	61 ± 4	67 ± 4
P_2	0.05 ± 0.01	0.05 ± 0.02
P_3 (mmHg)	98 ± 6	103 ± 6
P_4 (mmHg)	70 ± 4	65 ± 4
G_{max}	−0.8 ± 0.2	−0.8 ± 0.2

Values are means ± S.D. ($n = 8$). See eqn (1) in Methods for definition of the four parameters of the logistic function. All parameters were similar in supine and upright tilt positions.

halving the orthostatic activation of SNA (13 a.u. *versus* 25 a.u) and decreasing the operating AP at upright tilt by 10 mmHg compared with when the resetting is in operation. These findings support our second hypothesis that resetting of the arterial baroreflex contributes to preventing postural hypotension.

Our data indicate that resetting of the baroreflex neural arc contributes to preserving the baroreflex total arc function in an upright posture. In a simulation where resetting in the neural arc is absent, 60 deg upright tilt would shift the total arc downward to a lower AP (Fig. 5*D* and *E*) by a downward shift of the peripheral arc. However, in our experiments, 60 deg upright tilt maintained the total arc (Fig. 5*D* and *E*) by orthostatic resetting of the neural arc. These findings indicate that resetting of the neural arc has an important role in maintaining the total baroreflex function in an upright posture.

Little is known about the arterial baroreflex system under orthostatic stress. Although earlier studies addressed the baroreflex in relation to AP regulation under orthostatic stress, most of them evaluated the baroreflex in a supine, not orthostatic, position (Mosqueda-Garcia *et al.* 1997). In addition, although earlier studies investigated the gains of baroreflex control of SNA (Mosqueda-Garcia *et al.* 1997), vascular resistance (Cooper & Hainsworth, 2001) and R–R interval (Cooke *et al.* 1999), these gains were part of the total baroreflex system, and thus could not explain the operating points of the baroreflex. In the present study, we determined the neural and peripheral arcs independently in an upright position using the baroreflex open-loop equilibrium diagram. We found that upright tilt shifted the baroreflex neural arc to a higher SNA, while it shifted the baroreflex peripheral arc to a lower AP. Our data confirmed the accuracy of the equilibrium diagram in defining the operating point, since in both supine and upright tilt positions, the operating points estimated from the diagram agreed well with those measured in the baroreflex closed-loop condition (Fig. 6). This is consistent with earlier studies addressing haemorrhage (Sato *et al.* 1999) and muscle stretch (Yamamoto *et al.* 2004).

The mechanism responsible for the resetting of baroreflex neural arc with upright tilt remains unclear. The most likely mechanism is recruitment of other sympathoexcitatory systems than the baroreflex during orthostatic stress. In particular, the vestibular system is stimulated by upright tilt, and has been reported to increase SNA (vestibulosympathetic reflex) (Yates, 1992) and assist AP regulation during orthostatic stress in humans (Ray & Carter, 2003) and rats (Gotoh *et al.* 2004). In addition, contractions of the antigravity muscles during upright tilt stimulate the muscle reflexes that increase SNA (Potts & Mitchell, 1998; Yamamoto *et al.* 2004). Thus recruitments of other systems may shift the CSP–SNA relationship to a higher SNA.

However, the resetting of the baroreflex neural arc during upright tilt may not result from simple summation of SNA activation by the arterial baroreflex and by other systems. Theoretically, if the recruitments of other systems only offset SNA, it increases P_4 (the minimum value of SNA) but not P_1 (the range of SNA response to CSP) of the neural arc, and causes a parallel shift of the CSP–SNA relationship to a higher SNA without transforming the inverse sigmoid curve. In contrast, our results showed that 60 deg upright tilt increased not only P_4 but also P_1 (Table 2), and widened the inverse sigmoid curve. These findings suggest an interaction between baroreflex and

other systems in upright tilt posture. Indeed, the vestibular system has been considered to interact with the baroreflex (Yates, 1992; Kaufmann *et al.* 2002; Monahan & Ray, 2002; Ray & Carter, 2003; Gotoh *et al.* 2004). In addition, the muscle reflex has been reported to interact with the baroreflex (Potts & Mitchell, 1998), and contribute to the central resetting of the baroreflex during exercise (DiCarlo & Bishop, 2001; Miki *et al.* 2003). We have recently reported that passive stretch of the triceps surae muscles shifts the CSP–SNA relationship to a higher SNA using the baroreflex equilibrium diagram analysis (Yamamoto *et al.* 2004). Further studies are necessary to address the mechanism for the resetting during upright tilt.

Our data indicate that 60 deg upright tilt reduces the pressor response to SNA in the peripheral cardiovascular system. We observed that upright tilt down-shifted the baroreflex peripheral arc to a lower AP. For all SNA levels, AP was lower in the upright than supine position (Figs 4 and 5). This change may be attributed to the gravitational fluid shift toward the lower part of the body (i.e. abdominal vascular bed, lower limbs), which decreases the preload and effective circulatory blood volume (Sagawa *et al.* 1988; Rowell, 1993).

Our data suggest that upright tilt yields a different effect on the baroreflex system compared with haemorrhage. Haemorrhage decreases effective circulatory blood volume and preload (Sagawa *et al.* 1988; Rowell, 1993). Earlier study in rats demonstrated that haemorrhage (blood loss in the range of 0.5–2% of body weight) reduced AP in a prevailing level of SNA in the baroreflex peripheral arc (Sato *et al.* 1999), similar to our upright tilt. Therefore, both upright tilt and haemorrhage reduce the pressor response to SNA in the peripheral cardiovascular system. In contrast to upright tilt, haemorrhage did not affect the baroreflex neural arc (Sato *et al.* 1999). In short, upright tilt resets the baroreflex neural arc to a higher SNA whereas haemorrhage does not.

Since we focused on arterial baroreflex dynamics in response to an acute orthostatic stress, our findings could not relate long-term pressure regulation by arterial and cardiopulmonary baroreflexes and the renin–angiotensin system. Early study showed that chronic sino-aortic and cardiopulmonary denervations increased AP and activated the renin–angiotensin system in the conscious dog (Persson *et al.* 1988). Further study is needed to address long-term orthostatic physiology.

As we investigated the role of the arterial baroreflex in AP control under orthostatic stress while AP was well maintained, our findings could not explain the pathophysiology of orthostatic vasovagal syncope. Interestingly, the final trigger of human orthostatic syncope appears to be the abrupt disappearance of SNA (Morillo *et al.* 1997). Given the present findings, we speculate that some changes in the baroreflex neural arc can decrease SNA and trigger orthostatic syncope.

Limitations

The present study has several limitations. First, we excluded the efferent effect of vagally mediated arterial baroreflex, which could affect the properties of the two arcs. Second, we used an anaesthetic agent (intravenous injection of a mixture of urethane and α-chloralose) that could flatten the baroreflex peripheral arc by reducing the cardiac pumping function.

Third, since we measured only renal SNA, our findings have limited applicability to other SNA, including cardiac SNA. Although static regulation of the baroreflex neural arc over SNA is similar in renal and cardiac SNAs in

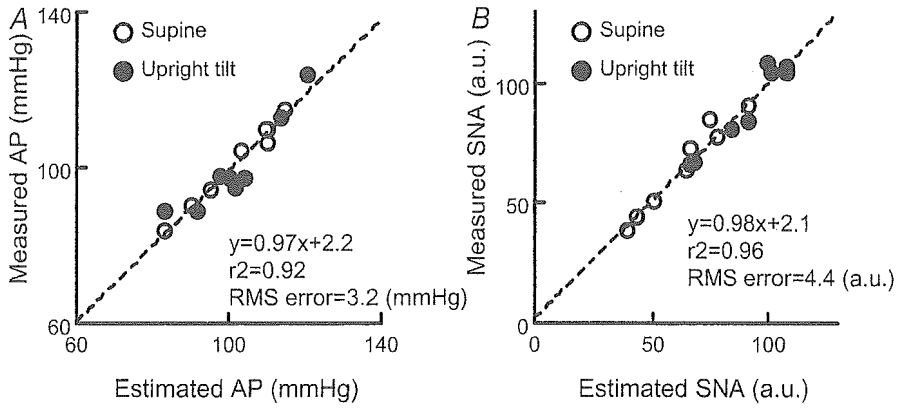

Figure 6. The relationship between the operating points estimated from the baroreflex open-loop equilibrium diagram (protocols 1 and 3) and those actually measured under the baroreflex closed-loop condition (protocol 2) in all animals ($n = 8$)

A and *B* show the operating AP and SNA, respectively. Each animal provided two data points obtained in supine (open circles) and upright tilt positions (filled circles). Both the operating AP and SNA estimated by the equilibrium diagram match the values actually measured under the baroreflex closed-loop condition. RMS: root mean square.

supine posture (Kawada *et al.* 2001), whether this holds true during orthostatic stress remains to be verified.

Fourth, we were not able to quantify the contribution of cardiac function (i.e. cardiac output) to AP regulation. Since the baroreflex peripheral arc represents the static relation from SNA input to AP, it includes the effects of SNA on cardiac function, stressed blood volume and vascular resistance. We were not able to isolate these factors because of complexity and experimental difficulties.

Fifth, we eliminated cardiopulmonary baroreflex by cutting bilateral vagal nerves. Earlier human studies have indicated that non-hypotensive hypovolaemic perturbations do not change AP, but reduce central venous, right heart and pulmonary pressures, and cause vasoconstriction. These observations have been interpreted as reflexes triggered by cardiopulmonary baroreceptors (Johnson *et al.* 1974; Pawelczyk & Raven, 1989). However, Taylor *et al.* (1995) showed that small reductions of effective blood volume reduce aortic baroreceptive areas and trigger haemodynamic adjustments which are so efficient that alterations in AP escape detection by conventional means. Accordingly, further studies are needed to understand the relative importance and mutual cooperation of arterial and cardiopulmonary baroreflexes in AP control during orthostatic stress.

Lastly, we used rabbits, which are quadrupeds. Since humans spend most of their time in nearly 90 deg upright postures whereas rabbits do not, our findings have limited applicability to humans. However, Japanese White rabbits spend most of their time in 10–40 deg head-up posture, and frequently stand up to nearly 70 deg. This suggests that rabbits have an ability to maintain arterial pressure against gravity-induced pressure perturbation under orthostatic stress. Additionally, in our preliminary experiments in rabbits, we observed that denervation of both carotid and aortic arterial baroreflexes caused postural hypotension of approximately 50 mmHg during 60 deg upright tilt, consistent with a previous study in rats (Sato *et al.* 2002). This suggests that even in quadrupeds, the arterial baroreflex has a very important role in the maintenance of AP under orthostatic stress. Accordingly, we speculate that our findings may reflect, at least, the qualitative aspects of orthostatic baroreflex physiology in humans. Indeed, recent human studies have suggested that orthostatic stress (lower body negative pressure) enhances the SNA response to arterial pressure change in the baroreflex closed-loop condition (Ichinose *et al.* 2004*a*; Ichinose *et al.* 2004*b*)

In conclusion, baroreflex open-loop equilibrium analysis demonstrated that 60 deg upright tilt shifted the baroreflex neural arc to a higher SNA and shifted the peripheral arc to a lower AP. Consequently, the upright tilt markedly increased the operating SNA and maintained the operating AP. Simulation study suggests that resetting of the neural arc would double the orthostatic activation of SNA and increase the operating AP in upright tilt by 10 mmHg compared with the absence of resetting. These data suggest that orthostatic stress increases SNA by resetting the baroreflex neural arc. The resetting of the neural arc may compensate for the reduced pressor responses to SNA in the peripheral cardiovascular system, and contribute to preventing postural hypotension.

References

Angell James JE (1971). The effects of changes of extramural, 'intrathoracic', pressure on aortic arch baroreceptors. *J Physiol* **214**, 89–103.

Cooke WH, Hoag JB, Crossman AA, Kuusela TA, Tahvanainen KU & Eckberg DL (1999). Human responses to upright tilt: a window on central autonomic integration. *J Physiol* **517**, 617–628.

Cooper VL & Hainsworth R (2001). Carotid baroreceptor reflexes in humans during orthostatic stress. *Exp Physiol* **86**, 677–681.

DiCarlo SE & Bishop VS (2001). Central baroreflex resetting as a means of increasing and decreasing sympathetic outflow and arterial pressure. *Ann N Y Acad Sci* **940**, 324–337.

Eckberg DL & Sleight P (1992). *Human Baroreflexes in Health and Disease*. Oxford University Press, New York.

Glantz SA (1997). *Primer of Biostatistics*, 4th edn. McGraw-Hill, New York.

Gotoh TM, Fujiki N, Matsuda T, Gao S & Morita H (2004). Roles of baroreflex and vestibulosympathetic reflex in controlling arterial blood pressure during gravitational stress in conscious rats. *Am J Physiol Regul Integr Comp Physiol* **286**, R25–R30.

Ichinose M, Saito M, Kitano A, Hayashi K, Kondo N & Nishiyasu T (2004*a*). Modulation of arterial baroreflex dynamic response during mild orthostatic stress in humans. *J Physiol* **557**, 321–330.

Ichinose M, Saito M, Ogawa T, Hayashi K, Kondo N & Nishiyasu T (2004*b*). Modulation of control of muscle sympathetic nerve activity during orthostatic stress in humans. *Am J Physiol Heart Circ Physiol* **287**, H2147–H2153.

Johnson JM, Rowell LB, Niederberger M & Eisman MM (1974). Human splanchnic and forearm vasoconstrictor responses to reductions of right atrial and aortic pressures. *Circ Res* **34**, 515–524.

Kaufmann H, Biaggioni I, Voustianiouk A, Diedrich A, Costa F, Clarke R, Gizzi M, Raphan T & Cohen B (2002). Vestibular control of sympathetic activity. An otolith-sympathetic reflex in humans. *Exp Brain Res* **143**, 463–469.

Kawada T, Shishido T, Inagaki M, Tatewaki T, Zheng C, Yanagiya Y, Sugimachi M & Sunagawa K (2001). Differential dynamic baroreflex regulation of cardiac and renal sympathetic nerve activities. *Am J Physiol Heart Circ Physiol* **280**, H1581–H1590.

Kawada T, Yanagiya Y, Uemura K, Miyamoto T, Zheng C, Li M, Sugimachi M & Sunagawa K (2003). Input-size dependence of the baroreflex neural arc transfer characteristics. *Am J Physiol Heart Circ Physiol* **284**, H404–H415.

Kent B, Drane J, Blumenstein B & Manning J (1972). A mathematical model to assess changes in the baroreceptor reflex. *Cardiology* **57**, 295–310.

Miki K, Yoshimoto M & Tanimizu M (2003). Acute shifts of baroreflex control of renal sympathetic nerve activity induced by treadmill exercise in rats. *J Physiol* **548**, 313–322.

Monahan KD & Ray CA (2002). Vestibulosympathetic reflex during orthostatic challenge in aging humans. *Am J Physiol Regul Integr Comp Physiol* **283**, R1027–R1032.

Morillo CA, Eckberg DL, Ellenbogen KA, Beightol LA, Hoag JB, Tahvanainen KU, Kuusela TA & Diedrich AM (1997). Vagal and sympathetic mechanisms in patients with orthostatic vasovagal syncope. *Circulation* **96**, 2509–2513.

Mosqueda-Garcia R, Furlan R, Fernandez-Violante R, Desai T, Snell M, Jarai Z, Ananthram V, Robertson RM & Robertson D (1997). Sympathetic and baroreceptor reflex function in neurally mediated syncope evoked by tilt. *J Clin Invest* **99**, 2736–2744.

Pawelczyk JA & Raven PB (1989). Reductions in central venous pressure improve carotid baroreflex responses in conscious men. *Am J Physiol* **257**, H1389–H1395.

Persson P, Ehmke H, Kirchheim H & Seller H (1988). Effect of sino-aortic denervation in comparison to cardiopulmonary deafferentiation on long-term blood pressure in conscious dogs. *Pflugers Arch* **411**, 160–166.

Persson P & Kirchheim H (1991). *Baroreceptor Reflexes: Integrative Functions and Clinical Aspects*. Springer-Verlag, Berlin.

Potts JT & Mitchell JH (1998). Rapid resetting of carotid baroreceptor reflex by afferent input from skeletal muscle receptors. *Am J Physiol* **275**, H2000–H2008.

Ray CA & Carter JR (2003). Vestibular activation of sympathetic nerve activity. *Acta Physiol Scand* **177**, 313–319.

Rea RF & Eckberg DL (1987). Carotid baroreceptor-muscle sympathetic relation in humans. *Am J Physiol* **253**, R929–R934.

Rowell LB (1993). *Human Cardiovascular Control*. Oxford University Press, New York.

Rudas L, Crossman AA, Morillo CA, Halliwill JR, Tahvanainen KU, Kuusela TA & Eckberg DL (1999). Human sympathetic and vagal baroreflex responses to sequential nitroprusside and phenylephrine. *Am J Physiol* **276**, H1691–H1698.

Sagawa K, Maughan L, Suga H & Sunagawa K (1988). *Cardiac Contraction and the Pressure-Volume Relationship*. Oxford University Press, New York.

Sato T, Kawada T, Inagaki M, Shishido T, Takaki H, Sugimachi M & Sunagawa K (1999). New analytic framework for understanding sympathetic baroreflex control of arterial pressure. *Am J Physiol* **276**, H2251–H2261.

Sato T, Kawada T, Sugimachi M & Sunagawa K (2002). Bionic technology revitalizes native baroreflex function in rats with baroreflex failure. *Circulation* **106**, 730–734.

Taylor JA, Halliwill JR, Brown TE, Hayano J & Eckberg DL (1995). 'Non-hypotensive' hypovalaemia reduces ascending aortic dimensions in humans. *J Physiol* **483**, 289–298.

Yamamoto K, Kawada T, Kamiya A, Takaki H, Miyamoto T, Sugimachi M & Sunagawa K (2004). Muscle mechanoreflex induces the pressor response by resetting the arterial baroreflex neural arc. *Am J Physiol* **286**, H1382–H1388.

Yates B (1992). Vestibular influence on the sympathetic nervous system. *Brain Res Brain Res Rev* **17**, 51–59.

Acknowledgements

This study was supported by Industrial Technology Research Grant Program, 03A47075, from New Energy and Industrial Technology Development Organization (NEDO) of Japan, by the Program for Promotion of Fundamental Studies in Health Science of the Organization for Pharmaceutical Safety and Research of Japan, and also by the Ground-based Research Announcement for Space Utilization promoted by Japan Space Forum.

Japanese Journal of Physiology, 55, 157–163, 2005

Dynamic Characteristics of Carotid Sinus Pressure-Nerve Activity Transduction in Rabbits

Toru KAWADA, Kenta YAMAMOTO, Atsunori KAMIYA, Hideto ARIUMI, Daisaku MICHIKAMI, Toshiaki SHISHIDO, Kenji SUNAGAWA*, and Masaru SUGIMACHI

Department of Cardiovascular Dynamics, Advanced Medical Engineering Center, National Cardiovascular Center Research Institute, Osaka, 565-8565 Japan; and *Department of Cardiovascular Medicine, Graduate School of Medical Sciences, Kyushu University, Fukuoka, 812-8582 Japan

Abstract: The dynamic characteristics of the baroreflex neural arc from pressure input to efferent sympathetic nerve activity (SNA) reveal derivative characteristics in the frequency range of 0.01 to 0.8 Hz (i.e., the baroreflex gain augments with increasing frequency) and high-cut characteristics in the frequency range above 0.8 Hz (i.e., the baroreflex gain decreases with increasing frequency) in rabbits. The derivative characteristics accelerate the arterial pressure regulation via the baroreflex. The high-cut characteristics preserve the baroreflex gain against pulsatile pressure by attenuating the high-frequency components less necessary for arterial pressure regulation. However, to what extent the carotid sinus baroreceptor transduction from pressure input to afferent baroreceptor nerve activity (BNA) contributes to these characteristics remains unanswered. To test the hypothesis that the carotid sinus pressure-BNA transduction partly explains the derivative characteristics but not the high-cut characteristics, we examined the dynamic BNA response to pressure input in the frequency range from 0.01 to 3 Hz by using a white noise analysis in 7 anesthetized rabbits. The transfer function from pressure input to BNA showed slight derivative characteristics in the frequency range from 0.01 to 0.3 Hz with approximately a 1.7-fold increase in dynamic gain, but it showed no high-cut characteristics. In conclusion, the carotid sinus baroreceptor transduction partly explained the derivative characteristics but not the high-cut characteristics of the baroreflex neural arc. The present results suggest the importance of the central processing from BNA to efferent SNA to account for the overall dynamic characteristics of the baroreflex neural arc. [The Japanese Journal of Physiology 55: 157–163, 2005]

Key words: systems analysis, transfer function, baroreflex neural arc.

The carotid sinus baroreflex is among the most important negative feedback systems that stabilize arterial pressure (AP) during daily activity. A knowledge of the dynamic characteristics of a given system is important for an in-depth understanding of the system behavior. In previous studies [1–4], we applied a white noise analysis to the carotid sinus baroreflex in rabbits and assessed the transfer function of the baroreflex neural arc from pressure input to efferent sympathetic nerve activity (SNA). The neural arc transfer function revealed two distinct features. One relates to the derivative characteristics in which the baroreflex gain augments with increasing frequency from 0.01 to 0.8 Hz. The derivative characteristics accelerate the dynamic AP regulation by the carotid sinus baroreflex [1]. The other feature relates to the high-cut characteristics in which the baroreflex gain decreases with increasing frequency above 0.8 Hz [4]. The high-cut characteristics prevent the high-frequency components from saturating the baroreflex central processing and preserve the baroreflex gain against pulsatile pressure. However, whether the carotid sinus

Received on Jun 30, 2005; accepted on Jul 29, 2005; released online on Aug 5, 2005; DOI: 10.2170/jjphysiol.R2122
Correspondence should be addressed to: Toru Kawada, Department of Cardiovascular Dynamics, Advanced Medical Engineering Center, National Cardiovascular Center Research Institute, 5-7-1 Fujishirodai, Suita, Osaka, 565-8565 Japan. Phone:+81-6-6833-5012 (Ext. 2427), Fax: +81-6-6835-5403, E-mail: torukawa@res.ncvc.go.jp

baroreceptor transduction from the pressure input to afferent baroreceptor nerve activity (BNA) or the central processing from the afferent BNA to efferent SNA played a major role in forming derivative and high-cut characteristics remains unanswered.

The dynamic characteristics of the pressure input-nerve activity transduction have been examined by the use of step and sinusoidal inputs [5–7]. Although these classical inputs and resulting outputs are easy to interpret, they have a critical drawback because only limited aspects of the system characteristics can be identified. In other words, the system response to untested input signals cannot be predicted precisely because the untested input signals may have frequency components that the step or sinusoidal input does not have. A white noise input, which is rich in frequency components, is most appropriate for a thorough examination of a given system [8–10]. We have identified the dynamic characteristics from pressure input to aortic depressor nerve activity in rabbits with the white noise analysis [11]. The results of that study suggest that the derivative characteristics of the baroreflex neural arc may be partly attributable to the pressure input-nerve activity transduction, whereas the high-cut characteristics may be primarily attributable to the central processing from BNA to efferent SNA. However, regional differences of the transduction properties have been reported between carotid sinus and aortic baroreceptors [12]. Hence the purpose of the present study was to directly estimate dynamic characteristics of the carotid sinus pressure (CSP)-BNA transduction by using the white noise analysis. The results confirmed the hypothesis that the CSP-BNA transduction partly explained the derivative characteristics, but not the high-cut characteristics.

METHODS

Surgical preparations. The animals were cared for in strict accordance with the Guiding Principles for the Care and Use of Animals in the Field of Physiological Sciences approved by the Physiological Society of Japan. Seven Japanese white rabbits weighing 2.7 to 3.1 kg were anesthetized by intravenous injection (2 ml/kg) of a mixture of urethane (250 mg/ml) and α-chloralose (40 mg/ml), and mechanically ventilated with oxygen-enriched room air. A supplemental dose of these anesthetics was administered continuously (0.5 $ml \cdot kg^{-1} \cdot h^{-1}$) to maintain an appropriate level of anesthesia. AP was monitored by a high-fidelity pressure transducer (Millar Instruments, Houston, TX) inserted via the right femoral artery. Following a midline cervical incision, the right external carotid artery was exposed, ligated at two positions, and sectioned in between to access the tissue between the external and internal carotid arteries. A carotid sinus nerve was identified by using a pair of platinum electrodes and by confirming AP-synchronous activity on a loudspeaker. The nerve was then freed from the platinum electrodes during the following carotid sinus isolation procedure. The right internal carotid artery and other small branches arising from the carotid sinus area were ligated. A catheter (0.6 mm internal diameter, 15 cm long) was introduced from the right common carotid artery, and the carotid sinus blind sac was filled with warmed physiological saline. CSP was measured at the end of the catheter opposite the carotid sinus and was controlled by a servo-controlled piston pump (model ET-126A, Labworks, Costa Mesa, CA). A small amount of leakage from the isolated carotid sinus, if any remained, was replenished from the pump during the experiment. After completing the carotid sinus isolation procedure, we attached a pair of stainless steel wire electrodes to the previously identified carotid sinus nerve (Bioflex wire AS633, Cooner Wire, CA) for the multifiber recording of BNA. The nerve and electrodes were secured with silicone glue (Kwik-Cast, World Precision Instruments, Inc.) for insulation. The preamplified nerve signal was band-pass filtered at 150–1,000 Hz. It was then full-wave rectified and low-pass filtered at 30 Hz to quantify the nerve activity. The left carotid sinus nerve, bilateral aortic depressor nerves, and bilateral vagal nerves were all sectioned. The body temperature of the experimental animal was maintained at approximately 38°C with a heating pad.

In three of the seven animals, the controlled CSP was compared with the actual pressure imposed on the carotid sinus area after the BNA recording experiment had finished. After carefully removing the electrodes and silicone glue, we loosened a ligature to the external carotid artery. A catheter-tip pressure transducer (Millar Instruments, Houston, TX) was then introduced into the carotid sinus from the external carotid artery. A signal from the transducer served as the actual pressure imposed on the isolated carotid sinus area.

Protocols. Random input protocol: We randomly changed CSP to either 80 or 120 mmHg with a switching interval of 50 ms for 15 min in order to estimate the dynamic characteristics of the CSP-BNA transduction.

Stepwise input protocol: We increased CSP from 20 to 180 mmHg every minute with a step size of 20

mmHg in order to estimate the static characteristics of the CSP-BNA transduction.

We recorded CSP, BNA and AP at a sampling rate of 200 Hz by using a 12-bit analog-to-digital converter. The data were stored on the hard disk of a dedicated laboratory computer system for later analysis.

Data analysis. In the random input protocol, we estimated the transfer function, $H(f)$, from CSP input to BNA output according to previous studies [1–4, 8, 10–11, 13]. We normalized the transfer function so that the average transfer gain value below 0.02 Hz became unity and expressed BNA in arbitrary units for dynamic analysis (AU_{dyn}). We also calculated the coherence function, $Coh(f)$, between CSP and BNA [1–4, 8, 10–11, 13]. A unity coherence value indicates perfect linear dependence whereas zero coherence value indicates total independence between CSP and BNA.

In the stepwise input protocol, we calculated the steady-state BNA values by averaging the data during the last 10 s of each CSP level. We then scaled these values so that their minimum and maximum BNA values became 0 and 100 arbitrary units (AU_{stat}), respectively, for static analysis. We performed a regression analysis for the four-parameter logistic function using Eq. 1 [14].

$$y = \frac{P_1}{1+\exp[P_2(x-P_3)]} + P_4 \qquad (1)$$

where P_1 is the response range (i.e., the difference between the maximum and minimum values of y), P_2 is the slope coefficient, P_3 is the midpoint on the input axis, and P_4 is the minimum value of y. The fitting error (err%) for the logistic function was evaluated by using Eq. 2.

$$err\% = \frac{\sum_{k=1}^{N}[u(k)-y(k)]^2}{\sum_{k=1}^{N}[u(k)-\bar{u}]^2} \times 100 \qquad (2)$$

where u(k) and y(k) indicate the measured and predicted BNA values at each CSP level. N indicates the number of data points analyzed, and $\bar{u}$ represents the average value of u(k) when k spans from 1 to N.

RESULTS

The dynamic characteristics of the pressure transduction from CSP to actual pressure imposed on the carotid sinus area are depicted in Fig. 1A. The gain plot (top panel) indicates the ratio of actual pressure to CSP in the frequency domain. The controlled CSP faithfully reflected the actual pressure up to 3 Hz. The ratio was greatly dispersed above 3 Hz. The phase plot (middle panel) indicates that the phase delay was negligible up to 1 Hz. The phase delay at 3 Hz was approximately 0.33 radians. The coherence plot (bottom panel) indicates that the coherence was unity up to 3 Hz and decreased slightly above 3 Hz.

Figure 1B shows a typical time series of CSP and BNA obtained from the random input protocol. CSP was changed according to a binary white noise sequence. BNA varied in response to the CSP input. When CSP was increased, BNA was increased, and vice versa.

Figure 1C illustrates the transfer function from CSP to BNA averaged from all animals. The gain plot (top), phase plot (middle) and coherence plot (bottom) are presented. In each plot the thick line indicates the mean value, and the thin lines indicate the mean ± SEM values. In the gain plot, the gain value at the lowest frequency was normalized to unity. The gain increased with increasing frequency from 0.01 to 0.3 Hz and showed a relatively constant value of approximately 1.7 up to 3 Hz. In the phase plot, the phase value led slightly in the frequency range from 0.01 to 0.2 Hz and close to zero radians from 0.2 to 1 Hz. Although the phase delayed above 1 Hz, the delay is most likely attributable to the phase delay between CSP and actual pressure shown in Fig. 1A. In the coherence plot, the coherence was approximately 0.6 at the lowest frequency and increased to 0.8 in the frequency range of 0.1 to 3 Hz.

Figure 2A depicts the typical time series of CSP and BNA obtained from the stepwise input protocol. The CSP and BNA data were resampled at 2 Hz for these panels. An increase in CSP increased BNA in the CSP range of 40 to 160 mmHg. When the BNA response to stepwise input was obvious, it was greater at the onset of pressure change and then decayed to the steady-state value. The steady-state BNA value was not necessarily greater at 40 mmHg than at 20 mmHg across the animals. The steady-state BNA value was not necessarily greater at 180 mmHg than at 160 mmHg.

Figure 2B illustrates the static input-output relationship between CSP and BNA averaged from all animals. The closed circles and error bars represent mean and mean ± SEM values of BNA at each CSP level, respectively. The solid curve indicates the logistic function constructed from the averaged parameters shown in Table 1.

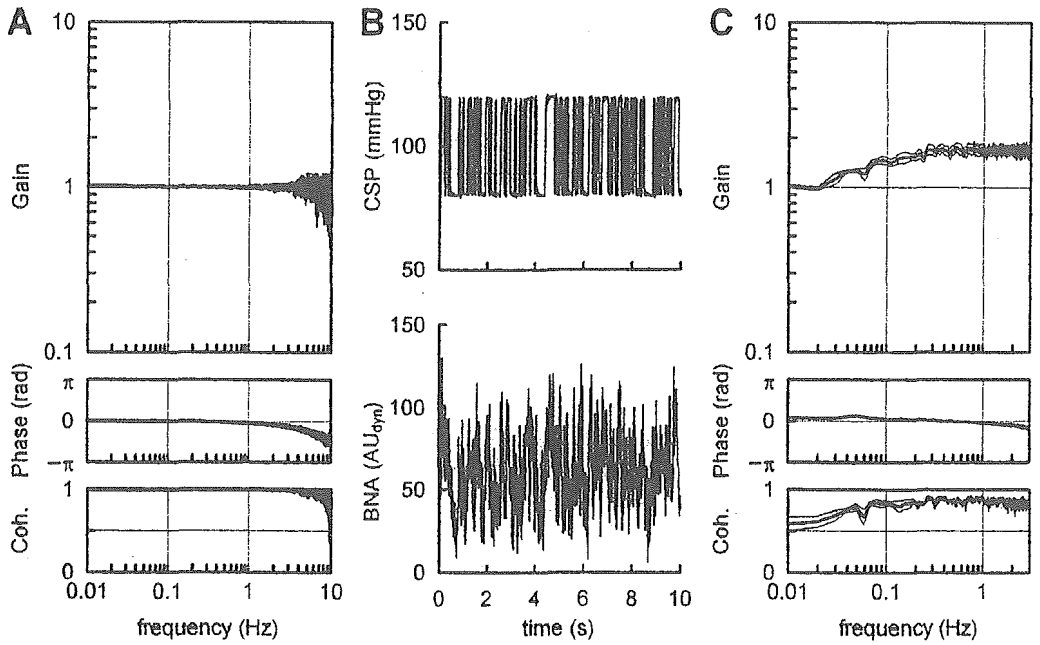

Fig. 1. A: The transfer function from controlled carotid sinus pressure (CSP) to actual pressure imposed on the carotid sinus area. The gain plot represents the ratio of actual pressure to CSP in the frequency domain. The phase plot represents the phase difference between CSP and actual pressure. The coherence (Coh.) shows the extent of linearity between CSP and actual pressure. Based on the transfer function from CSP to actual pressure, we employed the transfer function data up to 3 Hz in the analysis of CSP-nerve activity transduction. The phase difference between CSP and actual pressure in the frequency range between 1 and 3 Hz was taken into account in the interpretation of the CSP-nerve activity transduction. **B: Representative time series of CSP and afferent baroreceptor nerve activity (BNA) during the random input protocol.** CSP was changed according to a binary white noise signal with a switching interval of 50 ms. AU_{dyn}: arbitrary units for dynamic analysis. **C: Transfer function from CSP to BNA averaged from all animals.** The gain plot, phase plot, and coherence are shown. The transfer gain increased with increasing frequency from 0.01 to 0.3 Hz and showed a relatively constant value of approximately 1.7 up to 3 Hz. In all panels, thick and thin lines represent mean and mean ± SEM values.

Table 1 summarizes the parameters of the logistic function fitted to the steady-state CSP-BNA relationship obtained from the stepwise input protocol. The fitting error to the logistic function was less than 1% relative to the total variation in steady-state BNA values.

DISCUSSION

Dynamic characteristics of the carotid sinus baroreceptor transduction. Because of technical difficulty with the in situ preparation, we could not measure actual pressure imposed on the carotid sinus area and record BNA simultaneously. Therefore we measured controlled CSP and actual pressure imposed on the carotid sinus area simultaneously. As shown in Fig. 1A, the controlled CSP faithfully reflected the actual pressure up to 3 Hz. Above this frequency the ratio of actual pressure to CSP became greatly dispersed among animals. Because the compliance of the isolated area would depend on the vascular configuration and inevitably differ among animals, the pressure transduction in the frequencies above 3 Hz may reveal significant inter-individual differences. Actually, the insertion of the catheter-tip micromanometer itself might have affected the compliance of the isolated area to some degree. The phase delay reached approximately 0.33 radians at 3 Hz, which corresponds to 0.018 s of pure dead time. Although this value was not negligible, we employed the transfer function data up to 3 Hz in the analysis of the CSP-BNA relationship because the inter-individual differences in the phase delay were

Table 1. Parameters of the logistic function fitted to the steady-state CSP-BNA relationship.

Response range, P_1, AU_{stat}	98.1 ± 2.4
Slope coefficient, P_2, $mmHg^{-1}$	−0.072 ± 0.010
Midpoint pressure, P_3, mmHg	89.9 ± 3.4
Minimum value, P_4, AU_{stat}	0.05 ± 1.98
err%	0.9 ± 0.5

Data are means±SEM.

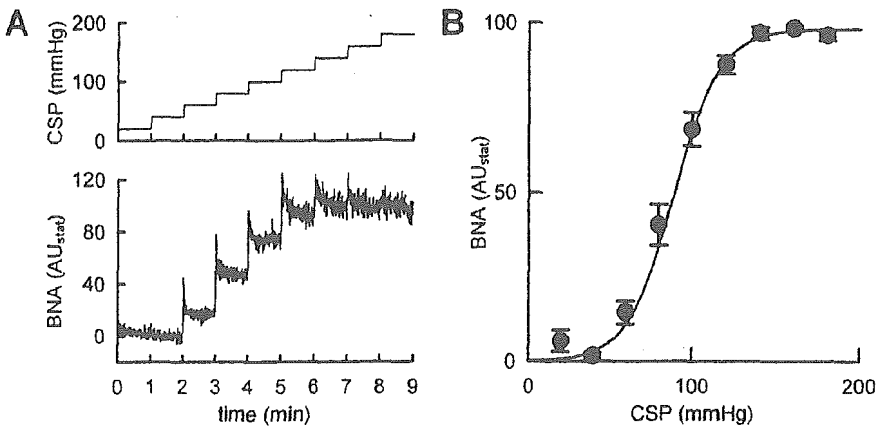

Fig. 2. A: Representative time series of carotid sinus pressure (CSP) and afferent baroreceptor nerve activity (BNA) during the stepwise input protocol. CSP and BNA were resampled at 2 Hz for the panels. CSP was increased from 20 to 180 mmHg every minute with a pressure step of 20 mmHg. **B: The CSP-BNA relationship averaged from all animals.** The CSP-BNA relationship revealed sigmoidal nonlinearity. The closed circles represent mean values, and the error bars indicate mean ± SEM values at each CSP. The solid curve indicates the logistic function derived from averaged parameters shown in Table 1. AU_{stat}: arbitrary units for static analysis.

very small up to 3 Hz. The phase delay between CSP and actual pressure should be taken into account in the interpretation of phase data of the transfer function from CSP to BNA shown in Fig. 1C. The phase delay between CSP and BNA noted in the frequency range above 1 Hz would be chiefly attributable to the phase delay between CSP and the actual pressure imposed on the carotid sinus area.

Derivative characteristics of the baroreflex neural arc contribute to the optimization of the AP regulation by the carotid sinus baroreflex [1]. Although Franz *et al.* [6] reported dynamic characteristics of single baroreceptor fiber activity in the rabbit carotid sinus in the frequency range from 0.078 to 2.5 Hz by using sinusoidal inputs, the derivative characteristics were obscure in that frequency range. As shown in Fig. 1C, dynamic gain from CSP to BNA augmented to approximately 1.7 with increasing frequency from 0.01 to 0.5 Hz, indicating the existence of the derivative characteristics. When the transfer function from CSP input to efferent SNA was identified in our previous study [15], dynamic gain increased to 3.8-fold for cardiac SNA and to 2.3-fold for renal SNA, with increasing frequency from 0.01 to 0.5 Hz (see Fig. 3 in Ref. 15). Thus approximately 40% (for cardiac) and 64% (for renal) of the derivative characteristic may be explained by the dynamic characteristics of the CSP-BNA transduction.

High-cut characteristics of the baroreflex neural arc attenuate high-frequency components in the input pressure and preserve the baroreflex gain against pulsatile pressure [4]. As shown in Fig. 1C, the dynamic gain of the transfer function from CSP to BNA was relatively constant in the frequency range from 0.3 to 3 Hz and showed no high-cut characteristics. Therefore the high-cut characteristics of the baroreflex neural arc are primarily attributable to the central processing from BNA to efferent SNA. In other words, the dynamic characteristics from BNA to efferent SNA should reveal high-cut characteristics with a corner frequency of approximately 0.8 Hz. The mechanism for the putative high-cut characteristics in the central processing remains unclear. The frequency-dependent depression of the signal transduction in the nucleus tractus solitarii (NTS) neurons [16] may be related to the upper frequency limit of central processing. However, the frequency-dependent depression refers to the phenomenon related to the stimulation frequency itself, whereas the high-cut characteristics refer to the attenuation of the system response related to the modulation frequency of the input. Further information is required to reconcile the putative high-cut characteristics and the frequency-dependent depression in the baroreflex central pathway.

The dynamic characteristics of the carotid sinus baroreceptor transduction were generally similar to those of the baroreceptor transduction of the aortic depressor nerve in rabbits [11]. However, a slight difference can be noted as follows. The gain increase from 0.01 to 0.1 Hz was approximately 1.7-fold (4.6 dB/decade) for the carotid sinus baroreceptors (Fig. 1C), whereas it was approximately 2-fold (6.0 dB/decade) for the aortic baroreceptors (see Fig. 5 in Ref. 11). In the rat aortic baroreceptor preparation, Brown *et al.* [5] demonstrated that myelinated fibers showed peaking in the frequency response, whereas unmyelinated fibers did not. The myelinated and unmyelinated fiber composition would affect the dynamic characteristics of multifiber BNA. Brown *et al.* [5] also demonstrated that the peaking of myelinated fiber response reached approximately 4 dB/decade in normotensive rats and approximately 6 dB/decade in spontaneously hyperten-

sive rats. Therefore the difference between the carotid sinus and aortic baroreceptor transductions, though it seems subtle, may reflect the difference in the myelinated and unmyelinated fiber composition and/or the difference in the prevailing pressure between the carotid sinus and aortic baroreceptors.

Static characteristics of the carotid sinus baroreceptor transduction. The static characteristics of the CSP-BNA transduction showed sigmoidal nonlinearity (Fig. 2B). BNA increased with CSP in the pressure range from 40 to 160 mmHg. In the single fiber preparation of the rabbit carotid sinus baroreceptors, the stimulus-response curve is fairly linear in each fiber between threshold pressure and saturation pressure [6]. However, the threshold pressure and the slope of the linear range vary considerably among fibers. Such variations in the static characteristics of single baroreceptor fiber activities are lumped together, possibly forming the sigmoidal relationship between CSP and multifiber BNA. The slope coefficient of the CSP-BNA relationship (Table 1) was smaller than the slope coefficient of the CSP-SNA relationship (0.10–0.12) determined in our previous studies [15, 17, 18]. In other words, the operating range of the system, which is inversely related to the slope coefficient [14], was wider for the CSP-BNA relationship than for the CSP-SNA relationship. The finding is consistent with our speculation, which is based on input-size and operating-point dependence of the baroreflex neural arc transfer function, that the static CSP-BNA relationship alone does not determine the overall nonlinearity of the neural arc characteristics [2, 3].

The midpoint pressure of the CSP-BNA relationship was approximately 90 mmHg, which is lower than the midpoint pressure of the CSP-SNA relationship (100–110 mmHg) determined in our previous studies [15, 17, 18]. The possibility cannot be ruled out, however, that the extensive surgical operation necessary for the BNA recording had altered the mechanical properties of the carotid sinus area differently from the preparation for the carotid sinus isolation alone. Although we had intended to simultaneously record afferent BNA and efferent SNA, the SNA and AP did not respond to the CSP input in the present experimental settings. A large portion of the baroreceptor afferent fibers may have been damaged because of fragility during the preparation. The difficulty results because we could not know, based on the magnitude of BNA, what percent of the nerve fibers were really kept intact. Further efforts are required to directly demonstrate the difference in the static input-output characteristics between the CSP-BNA relationship and the CSP-SNA relationship.

In conclusion, although a slight difference was noted, the dynamic characteristics of the carotid sinus baroreceptor transduction were similar to those of the aortic baroreceptor transduction in rabbits. The CSP-BNA transduction partly explained the derivative characteristics, but not the high-cut characteristics found in the neural arc transfer function from CSP to efferent SNA. The present results suggest the importance of the central processing from BNA to efferent SNA to account for the overall dynamic characteristics of the baroreflex neural arc.

This study was supported by the Health and Labour Sciences Research Grant for Research on Advanced Medical Technology from the Ministry of Health Labour and Welfare of Japan (H14-Nano-002), and by the Program for Promotion of Fundamental Studies in Health Science of the Pharmaceuticals and Medical Devices Agency of Japan.

REFERENCES

1. Ikeda Y, Kawada T, Sugimachi M, Kawaguchi O, Shishido T, Sato T, Miyano H, Matsuura W, Alexander J Jr, and Sunagawa K: Neural arc of baroreflex optimizes dynamic pressure regulation in achieving both stability and quickness. Am J Physiol Heart Circ Physiol 271: H882–H890, 1996
2. Kawada T, Uemura K, Kashihara K, Kamiya A, Sugimachi M, and Sunagawa K: A derivative-sigmoidal model reproduces operating point-dependent baroreflex neural arc transfer characteristics. Am J Physiol Heart Circ Physiol 286: H2272–H2279, 2004
3. Kawada T, Yanagiya Y, Uemura K, Miyamoto T, Zheng C, Li M, Sugimachi M, and Sunagawa K: Input-size dependence of the baroreflex neural arc transfer characteristics. Am J Physiol Heart Circ Physiol 284: H404–H415, 2003
4. Kawada T, Zheng C, Yanagiya Y, Uemura K, Miyamoto T, Inagaki M, Shishido T, Sugimachi M, and Sunagawa K: High-cut characteristics of the baroreflex neural arc preserve baroreflex gain against pulsatile pressure. Am J Physiol Heart Circ Physiol 282: H1149–H1156, 2002
5. Brown AM, Saum W, and Yasui S: Baroreceptor dynamics and their relationship to afferent fiber type and hypertension. Circ Res 42: 694–702, 1978
6. Franz GN, Sher AM, and Ito CS: Small signal characteristics of carotid sinus baroreceptors of rabbits. J Appl Physiol 30: 527–535, 1971
7. Spickler JW and Kezdi P: Dynamic response characteristics of carotid sinus baroreceptors. Am J Physiol 212: 472–476, 1967
8. Marmarelis PZ and Marmarelis VZ: Analysis of Physiological Systems, Plenum, New York, pp 131–221, 1978
9. Kawada T, Fujiki N, and Hosomi H: Systems analysis of the carotid sinus baroreflex system using a sum-of-sinusoidal input. Jpn J Physiol 42: 15–34, 1992
10. Sugimachi M, Imaizumi T, Sunagawa K, Hirooka Y, Todaka K, Takeshita A, and Nakamura M: A new method

to identify dynamic transduction properties of aortic baroreceptors. Am J Physiol Heart Circ Physiol 258: H887–H895, 1990
11. Sato T, Kawada T, Shishido T, Miyano H, Inagaki M, Miyashita H, Sugimachi M, Knuepfer MM, and Sunagawa K: Dynamic transduction properties of in situ baroreceptors of rabbits aortic depressor nerve. Am J Physiol Heart Circ Physiol 274: H358–H365, 1998
12. Pelletier CL, Clement DL, and Shepherd JT: Comparison of afferent activity of canine aortic and sinus nerves. Circ Res 31: 557–568, 1972
13. Bendat J and Piersol A: Random Data 3rd Ed. John Wiley & Sons, New York, pp 189–271, 2000
14. Kent BB, Drane JW, Blumenstein B, and Manning JW: A mathematical model to assess changes in the baroreceptor reflex. Cardiology 57: 295–310, 1972
15. Kawada T, Shishido T, Inagaki M, Tatewaki T, Zheng C, Yanagiya Y, Sugimachi M, and Sunagawa K: Differential dynamic baroreflex regulation of cardiac and renal sympathetic nerve activities. Am J Physiol Heart Circ Physiol 280: H1581–H1590, 2001
16. Liu Z, Chen C, and Bonham AC: Frequency limits on aortic baroreceptor input to nucleus tractus solitarii. Am J Physiol Heart Circ Physiol 278: H577–H585, 2000
17. Kawada T, Uemura K, Kashihara K, Jin Y, Li M, Zheng C, Sugimachi M, and Sunagawa K: Uniformity in dynamic baroreflex regulation of left and right cardiac sympathetic nerve activities. Am J Physiol Regul Integr Comp Physiol 284: R1506–R1512, 2003
18. Yamamoto K, Kawada T, Kamiya A, Takaki H, Miyamoto T, Sugimachi M, and Sunagawa K: Muscle mechanoreflex induces the pressor response by resetting the arterial baroreflex neural arc. Am J Physiol Heart Circ Physiol 286: H1382–H1388, 2004

Circ J 2005; **69:** 1527–1534

Assessment of Quality of Life With 5 Different Scales in Patients Participating in Comprehensive Cardiac Rehabilitation After Acute Myocardial Infarction

Shoji Suzuki, MD; Hiroshi Takaki, MD; Yoshio Yasumura, MD; Satoru Sakuragi, MD; Shuichi Takagi, MD; Yoshiaki Tsutsumi, MD; Naohiko Aihara, MD; Fumio Sakamaki, MD; Yoichi Goto, MD

Background Measures assessing quality of life (QOL) in patients participating in comprehensive cardiac rehabilitation (CCR) have not been established in Japan.

Methods and Results To compare different types of QOL scales and to determine the impact of CCR on QOL in Japanese cardiac patients, 5 different types of questionnaires were assessed in 44 patients participating in CCR after acute myocardial infarction (AMI). After 3-month CCR, peak oxygen uptake ($P\dot{V}O_2$, $p<0.01$), Sickness Impact Profile (SIP) total score ($p<0.05$) and physical function-related QOL scores (Specific Activity Scale (SAS), $p<0.01$; SIP physical score, $p<0.01$) significantly improved, whereas psychosocial/mental aspect-related QOL scores (Ministry of Health and Welfare (MHW)-QOL score, SIP psychosocial score, State-Trait Anxiety Inventory, Self-rating Depression Scale) did not change on the average. However, patients with low $P\dot{V}O_2$ ($<21.7\ ml \cdot min^{-1} \cdot kg^{-1}$) showed significant improvements in all scores after CCR, whereas patients with preserved exercise capacity showed improvements only in physical function-related scores (SAS and physical SIP). Furthermore, patients with anxiety and depression showed significant improvements in these respective measures after CCR.

Conclusion In patients with AMI, physical function-related QOL scores improve after a 3-month CCR program, but psychosocial/mental aspect-related QOL scores improve only in those with impaired exercise tolerance or anxiety/depression. Thus, changes in QOL after CCR depend on type of QOL scale used and the baseline status of the patient. In addition, in Japanese cardiac patients MHW-QOL mainly reflects psychosocial/mental aspect-related QOL, as well as overall QOL. (*Circ J* 2005; **69:** 1527–1534)

Key Words: Acute myocardial infarction; Cardiac rehabilitation; Depression; Psychological wellbeing; Quality of life

Comprehensive cardiac rehabilitation (CCR) improves psychological well-being or quality of life (QOL) in patients after acute myocardial infarction (AMI),[1–4] but because the various QOL scales assess the physical and psychological aspects of QOL differently, it is not fully understood which aspect of QOL is improved by CCR. In addition, it remains unclear which patient group benefits most from CCR in terms of QOL. Furthermore, because most QOL instruments, except for the QOL score of the Ministry of Health and Welfare in Japan (MHW-QOL),[5,6] were devised in Western countries, their features have not been comparably determined in Japanese cardiac patients. In fact, conflicting results have been reported on the effect of CCR on the MHW-QOL score in Japanese patients after AMI; Yoshida et al reported a significant improvement in the MHW-QOL score[6] whereas Fujiwara et al reported no significant change.[7]

The effect of CCR on the different aspects of QOL in Japanese patients after AMI using multiple QOL instruments has not been intensively assessed. Accordingly, the purpose of the present study was to use multiple QOL instruments to assess Japanese patients after AMI, to determine the comparative features of the various QOL scales, including the MHW-QOL score, and to clarify the characteristics of the patients who are likely to benefit most from CCR in terms of QOL.

(Received May 2, 2005; revised manuscript received September 29, 2005; accepted October 6, 2005)

Division of Cardiology, National Cardiovascular Center, Suita, Japan

Mailing address: Yoichi Goto, MD, Division of Cardiology, National Cardiovascular Center, 5-7-1 Fujishiro-dai, Suita 565-8565, Japan. E-mail: ygoto@hsp.ncvc.go.jp

Methods

Subjects

We studied 44 patients who had experienced an AMI (mean age: 58±9 years, range 45–78, male/female: 37/7) and who participated in CCR with exercise training program. All patients gave written informed consent.

The diagnosis of AMI was confirmed by electrocardiographic changes and serum creatine kinase (CK) elevation. Peak serum CK was 3,255±2,588 U/L. Seven patients (16%) had had a prior myocardial infarction and 2 patients (5%) had congestive heart failure (Killip's class ≥2) on admission. All patients underwent cardiac catheterization: 38 patients (86%) had successful percutaneous coronary intervention (PCI), 2 patients (5%) underwent coronary artery bypass grafting (CABG) and 5 patients (11%) with residual myocardial ischemia were medically controlled. Mean left ventricular ejection fraction (LVEF) was 45±8%

by left ventriculography 3–4 weeks after the onset of AMI.

Cardiac Rehabilitation Program

The CCR program consisted of exercise training of moderate intensity and education for 3 months, as previously described[8–10] Patients who did not have angina or ischemic changes on ECG at a low level of exercise (200–500 m walking test) were enrolled in the exercise training approximately 10–15 days after AMI. Patients with uncontrolled heart failure and/or angina, multiple organ disorders such as serum creatinine ≥2.0 mg/ml, serum transaminase ≥40 IU/ml, inflammatory disease or embolic disorders were excluded. The exercise program consisted of walking, bicycling on an ergometer, and aerobic dance sessions of 50–80 min, 3–5 times each week for 3 months. Exercise intensity was determined individually at 50–60% of heart rate reserve (Karvonen's equation, k=0.5–0.6)[11,12] obtained by maximal symptom-limited cardiopulmonary exercise testing (CPX) or at level 13 ("a little hard") of the 6–20 scale perceived rating of exercise (original Borg's score)[13] The exercise program started with supervised sessions for 2 weeks, followed by home exercise combined with once or twice weekly supervised sessions for the remaining 10 weeks. Home exercise consisted mainly of brisk walking at a prescribed heart rate for 30–60 min 3–5 times per week. There were no adverse cardiac events such as death, AMI, unplanned PCI or CABG, or worsening of heart failure during the 3-month CCR.

Patients were encouraged to attend the education classes, which were held 3 times each week with lectures on coronary artery disease, secondary prevention, diet, smoking cessation, medication, and home exercise given by physicians, nurses, dieticians, pharmacists and exercise instructors. In addition, all patients received individual counseling on exercise prescription, secondary prevention, and daily life activities by a physician and a CCR nurse at the time of hospital discharge and at the end of the CCR program.

CPX

A symptom-limited CPX was performed at the beginning and end of the 3-month CCR[14] After a 2 min rest on the bicycle ergometer (Examiner, Lode B.V. Groningen-Holland), patients started pedaling at an intensity of 0 W for 1 min (warm-up), then performed an incremental exercise test with a ramp protocol (15 W/min) until exhaustion. During exercise testing, breathed gas was continuously collected to measure oxygen uptake ($\dot{V}O_2$) and carbon dioxide production ($\dot{V}CO_2$) with a gas analyzer AE280 (Minato Medical Electronics, Osaka, Japan). Blood pressure was measured every minute and a 12-lead ECG was continuously monitored during exercise. Patients who showed angina or ischemic ECG changes at the initial exercise test were excluded.

Peak oxygen uptake ($P\dot{V}O_2$) was defined as the highest $\dot{V}O_2$ value achieved at peak exercise after reaching the respiratory compensation point. The $\dot{V}O_2$ value at the anaerobic threshold (AT) or ventilatory threshold was determined as the point at which $\dot{V}CO_2$ increased in a nonlinear fashion relative to the rate of $\dot{V}O_2$, according to the time trend of the ratio of minute ventilation ($\dot{V}_E$) and $\dot{V}O_2$ ($\dot{V}_E/\dot{V}O_2$), an abrupt increase in the respiratory exchange ratio, or the V-slope method[15,16]

QOL Questionnaires

At the beginning and end of the 3-month CCR program, all patients answered the 5 types of questionnaires assessing QOL: Specific Activity Scale (SAS), Sickness Impact Profile (SIP), MHW-QOL, State-Trait Anxiety Inventory (STAI) and Self-rating Depression Scale (SDS). SAS is a scale of functional capacity related to daily activities expressed by metabolic equivalents[17,18] and SIP comprises 136 items including 12 domains to assess patient behaviors, such as physical disorders (ambulation, mobility, body care and movement), psychosocial disorders (social interaction, alertness behavior, emotional behavior, communication) and other disorders (sleep and rest, eating, work, home management, recreation and pastimes), expressed by the percentage of acquired scores[19,20] It has been successfully used in the field of CCR[20–22] MHW-QOL has both generic and disease-related scales and mainly assesses the psychosocial and mental aspects of QOL[5–7] It comprises 39 items, including 3 domains (2 generic domains and 1 disease-specific domain) for subjective evaluation of health (8 items), social attitude and subjective wellbeing (21 items), and disease-specific conditions (10 items). In the present study we used a total score for the 39 items (so-called "broad sense score") as the MHW-QOL score. STAI is a scale of anxiety and comprises 2 domains of state-anxiety and trait-anxiety, the former representing an anxiety state that a patient faces and the latter mainly representing an anxious personality. Each domain comprises 20 items with 4-point scales[23] SDS evaluates depression by 20 items with 4-point scales[24] A state of anxiety and/or depression was judged when the percent score of STAI and/or SDS was above 50%. Higher scores indicate a more favorable QOL trait in SAS and MHW-QOL, whereas lower scores indicate a more favorable QOL trait in SIP, STAI and SDS.

Data Analysis

Data were analyzed in 3 steps. First, data for exercise capacity and QOL were compared between the 2 time points (ie, before and after the 3-month CCR) in the whole group of patients. Second, to assess the influence of baseline exercise capacity on the improvement in QOL scores after CCR, QOL data were compared between the 2 time points in the subgroups of preserved and impaired exercise capacity. Because the average $P\dot{V}O_2$ measured by CPX at the beginning of the CCR was 21.7±1.7 ml·min^{-1}·kg^{-1}, patients were divided into 2 groups according to their initial $P\dot{V}O_2$ value: Low $P\dot{V}O_2$ group ($P\dot{V}O_2$ <21.7 ml·min^{-1}·kg^{-1}, n=22) and Preserved $P\dot{V}O_2$ group ($P\dot{V}O_2$ ≥21.7 ml·min^{-1}·kg^{-1}, n=22). Finally, QOL data were compared between the 2 time points in the subgroups with and without initial anxiety (STAI score ≥50% or <50%, respectively) and with and without initial depression (SDS score ≥50% or <50%, respectively).

Statistical Analysis

All values are expressed as mean±SD. The paired t-test was used to compare paired variables before and after CCR within a group. Comparisons between groups were made by unpaired t-test. Statistical analysis was performed using StatView software (Abacus, Cupertino, CA, USA). A p-value less than 0.05 was considered statistically significant.

Results

Changes in Exercise Capacity and QOL Scores in the Whole Group

As shown in Table 1, which summarizes the baseline

Table 1 Characteristics of 44 Patients After Acute Myocardial Infarction

	Total (n=44)	Preserved $P\dot{V}O_2$ group (n=22)	Low $P\dot{V}O_2$ group (n=22)	p value
Age (years)	58±10	57±11	59±9	NS
Sex (M/F)	37/7	20/2	17/5	NS
Hypertension	21 (48%)	12 (55%)	9 (41%)	NS
Hyperlipidemia	18 (41%)	10 (45%)	8 (36%)	NS
Diabetes mellitus	12 (27%)	6 (27%)	6 (27%)	NS
Obesity (BMI ≥26 kg/m^2)	10 (23%)	4 (18%)	6 (27%)	NS
Smoking	23 (52%)	14 (64%)	9 (41%)	NS
Family history	9 (20%)	4 (18%)	5 (23%)	NS
Killip class ≥2 (numbers)	2	0	2	NS
PCI/CABG/none	38/2/5	18/1/3	20/1/2	NS
peak CK (IU/ml)	3,255±2,588	3,009±1,986	3,384±2,796	NS
LVEF (%)	44.5±8.2	45.9±6.6	42.9±9.6	<0.05
$P\dot{V}O_2$ (ml·kg^{-1}·min^{-1})	21.7±4.9	24.7±3.6	18.1±3.8	<0.001

Values are mean±SD. P values for comparisons between Preserved $P\dot{V}O_2$ and Low $P\dot{V}O_2$ groups.
$P\dot{V}O_2$, peak oxygen uptake; Preserved $P\dot{V}O_2$ group, patients whose baseline $P\dot{V}O_2$ values were equal to or above average ($P\dot{V}O_2$ ≥21.7 ml·kg^{-1}·min^{-1}); Low $P\dot{V}O_2$ group, patients whose baseline $P\dot{V}O_2$ value were below average ($P\dot{V}O_2$ <21.7 ml·kg^{-1}·min^{-1}); BMI, body mass index; PCI, percutaneous coronary intervention; CABG, coronary artery bypass grafting; CK, serum concentration of creatine kinase; LVEF, left ventricular ejection fraction.

Table 2 Exercise Capacity and QOL Scores Before and After Comprehensive Cardiac Rehabilitation in All Patients

	Before CCR	After CCR	p value
Peak R	1.26±0.12	1.24±1.0	NS
$P\dot{V}O_2$ (ml·kg^{-1}·min^{-1})	21.7±1.7	24.7±2.6	<0.01
$\dot{V}O_2$ at AT (ml·kg^{-1}·min^{-1})	11.8±2.3	13.1±2.5	<0.01
SAS (METs)	4.5±1.7	5.3±0.7	<0.05
SIP (% scores)			
Total	7.9±5.6	5.5±4.9	<0.05
Physical disorders	7.2±3.1	1.5±1.6	<0.01
Psychosocial disorders	6.0±4.4	5.8±7.4	NS
Other disorders	11.5±7.5	10.6±8.4	NS
MHW-QOL (scores)	57.4±12.7	58.6±20.5	NS
STAI (% scores)			
Total	49.3±10.9	46.9±13.2	NS
State-anxiety	48.2±11.7	45.3±12.2	NS
Trait-anxiety	49.7±12.0	47.1±12.3	NS
SDS (% scores)	45.3±9.5	43.4±7.9	NS

Values are mean±SD.
QOL, quality of life; CCR, comprehensive cardiac rehabilitation; Peak R, respiratory exchange ratio at peak exercise; $P\dot{V}O_2$, peak oxygen uptake; AT, anaerobic threshold (or ventilatory threshold); SAS, specific activity scale; METs, metabolic equivalents; SIP, sickness impact profile; MHW-QOL, QOL score of the Ministry of Health and Welfare in Japan; STAI, state-trait anxiety inventory; SDS, self-rating depression scale.

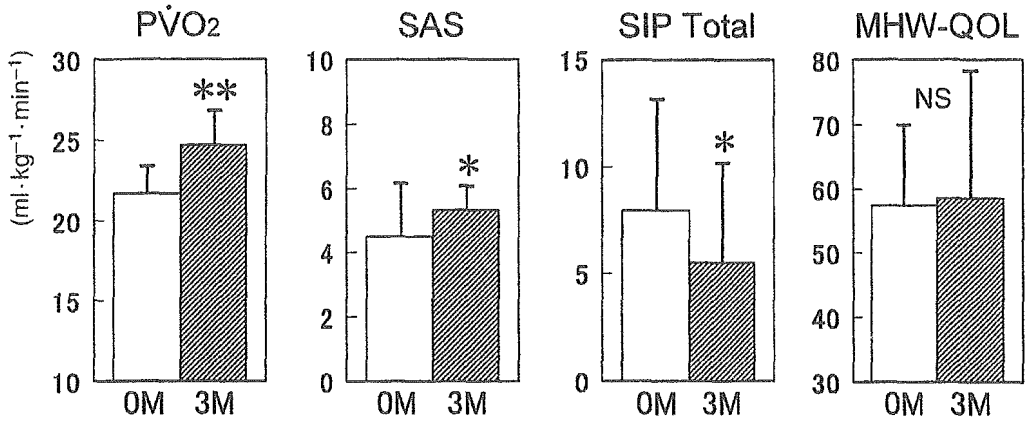

Fig 1. Comparisons of exercise capacity and quality of life (QOL) scores before and after 3-month comprehensive cardiac rehabilitation (CCR) in all 44 patients. $P\dot{V}O_2$, peak oxygen uptake; SAS, Specific Activity Scale; SIP total, Sickness Impact Profile total score; MHW-QOL, Ministry of Health and Welfare QOL broad sense score: 0M, baseline values (before CCR); 3M, values after 3-month CCR program. *p<0.05 and **p<0.01 compared with baseline values.

Table 3 Exercise Tolerance and QOL Related Scores Change in Subgroups

	Preserved $P\dot{V}O_2$ group (n=22)			*Low $P\dot{V}O_2$ group (n=22)*		
	Before CCR	*After CCR*	*p value#*	*Before CCR*	*After CCR*	*p value#*
$P\dot{V}O_2$ ($ml \cdot kg^{-1} \cdot min^{-1}$)	*24.7±3.6*	*27.5±5.0*	*<0.01*	*18.1±3.8***	*21.3±5.4***	*<0.01*
$\dot{V}O_2$ at AT ($ml \cdot kg^{-1} \cdot min^{-1}$)	*13.2±1.8*	*14.5±2.3*	*0.05*	*10.2±1.7*	*11.6±1.8*	*<0.05*
SAS (METs)	*5.0±1.7*	*5.6±1.9*	*<0.05*	*3.9±1.5**	*4.9±1.3*	*<0.05*
SIP (% scores)						
Total	*7.7±5.8*	*6.0±4.8*	*<0.05*	*8.1±5.6*	*4.1±5.2*	*<0.05*
Physical disorders	*6.9±7.9*	*0.8±1.7*	*<0.01*	*6.8±5.8*	*2.1±3.4*	*<0.01*
Psychosocial disorders	*6.2±6.9*	*6.6±7.6*	*NS*	*4.8±5.5*	*2.7±5.6*	*<0.05*
Other disorders	*10.5±6.2*	*10.6±8.1*	*NS*	*12.7±8.8*	*8.6±7.9*	*<0.05*
MHW-QOL (scores)	*61.0±8.1*	*60.3±10.8*	*NS*	*53.1±10.0***	*56.6±9.3*	*<0.05*
STAI (% scores)						
Total	*47.7±10.1*	*47.9±15.3*	*NS*	*51.2±11.8*	*45.7±10.3*	*<0.05*
State-anxiety	*47.9±10.3*	*47.6±17.0*	*NS*	*49.6±13.2*	*44.4±10.3*	*<0.05*
Trait-anxiety	*47.6±11.1*	*48.3±14.7*	*NS*	*52.7±12.6*	*46.9±11.2*	*<0.05*
SDS (% scores)	*42.3±7.0*	*43.6±10.7*	*NS*	*49.2±10.5**	*44.4±6.7*	*<0.05*

Values are mean±SD.
*#Comparisons were made by paired t-test before and after CCR within the group; *p<0.05, **p<0.01 compared with corresponding values in the Preserved $P\dot{V}O_2$ group.*
Abbreviations as in Table 2.

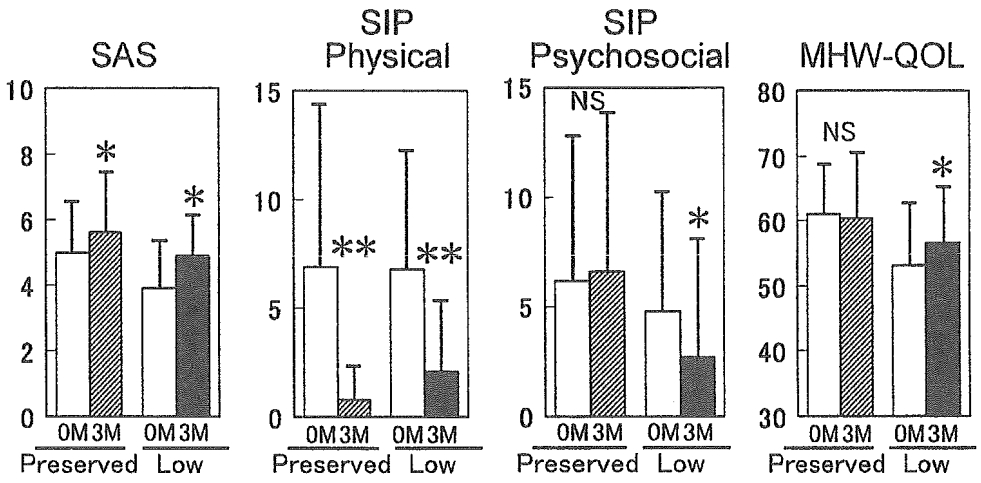

Fig 2. Changes in representative quality of life (QOL) scores before and after 3-month comprehensive cardiac rehabilitation program in patients with preserved and impaired exercise capacity. Patients with preserved exercise capacity showed improvements in Specific Activity Scale (SAS) and Sickness Impact Profile (SIP) physical score, but not in SIP psychosocial and Ministry of Health and Welfare (MHW)-QOL scores, whereas patients with impaired exercise capacity showed improvements in all 4 scores. SIP physical, SIP physical disorder score; SIP psychosocial, SIP psychosocial disorder score; Preserved, preserved exercise capacity group (peak $\dot{V}O_2$ ≥21.7 $ml \cdot min^{-1} \cdot kg^{-1}$); Low, impaired exercise capacity group (peak $\dot{V}O_2$ <21.7 $ml \cdot min^{-1} \cdot kg^{-1}$). *p<0.05 and **p<0.01 compared with baseline values.

clinical characteristics of the 2 groups with preserved and impaired exercise capacity, there were no significant differences except for LVEF and $P\dot{V}O_2$. Table 2 and Fig 1 summarize the data for exercise capacity and QOL scores before and after the 3-month CCR. The respiratory exchange ratio at peak exercise was sufficiently high both before and after CCR, suggesting that the measured $P\dot{V}O_2$ values are reliable. After 3 months of CCR, $P\dot{V}O_2$ (+13.8%, p<0.01), $\dot{V}O_2$ at AT (+11.0%, p<0.01) and SIP total score (–30.4%, p<0.05) improved significantly, as did the SAS (+17.8%, p<0.05) and SIP physical disorder score (–79.2%, p<0.01), both representing QOL related to physical function. However, other QOL scores such as the SIP score for psychosocial disorders and other disorders, MHW-QOL, STAI and SDS, all representing QOL related to psychosocial or mental function, did not change after 3 months of CCR.

Changes in QOL Scores in the Subgroups With Preserved and Impaired Exercise Capacity (Table 3, Fig 2)

In the Preserved $P\dot{V}O_2$ group, $P\dot{V}O_2$ (+11.3%, p<0.01), $\dot{V}O_2$ at AT (+9.8%, p=0.05), SIP total score (–22.1%, p< 0.05), and physical function-related QOL scores (ie, SAS (+12.0%, p<0.05) and SIP physical disorder score (–88.4%, p<0.01), significantly improved after CCR, but there was no significant change in the psychosocial and mental aspect-related QOL scores (ie, SIP psychosocial disorder score, SIP other disorder score, MHW-QOL, STAI, and SDS). In contrast, the Low $P\dot{V}O_2$ group showed significant improvements in $P\dot{V}O_2$ (+17.7%, p<0.01), $\dot{V}O_2$ at AT (+13.7%, p< 0.05), SIP total score (–49.4%, p<0.05), and both physical function-related QOL (SAS +25.6%, p<0.05; SIP physical disorder score –69.1%, p<0.01) and psychosocial/mental aspect-related QOL scores after CCR (SIP psychosocial disorder score –43.8%, p<0.05; MHW-QOL +6.7%, p<0.05;

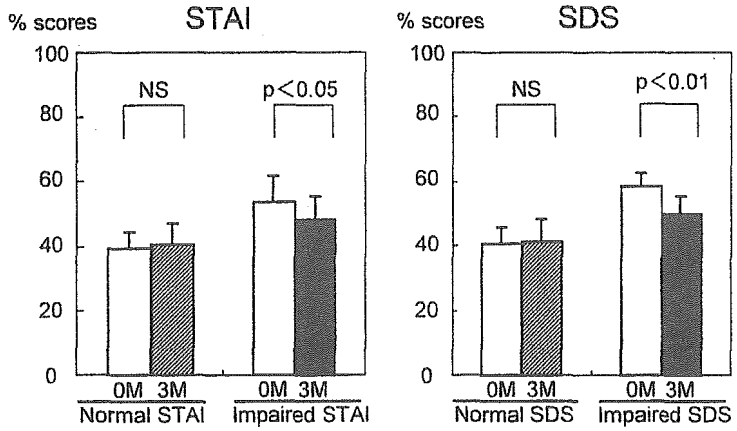

Fig 3. Changes in anxiety (STAI) and depression (SDS) scores before and after 3-month comprehensive cardiac rehabilitation (CCR) program in patients with normal and impaired mental function. Anxiety scores (STAI: State-Trait Anxiety Inventory) and depression scores (SDS: Self-rating Depression Scale) improved after CCR only in patients with impaired STAI score and impaired SDS score at baseline. 0M, baseline values (before CCR); 3M, values after 3-month CCR. *p<0.05 and **p<0.01 compared with baseline values.

Table 4 Correlation Matrix of Different Types of QOL Scores

	$P\dot{V}O_2$	$\dot{V}O_2$ at AT	SAS	SIP total	SIP physical	SIP psychosocial	STAI	SDS
MHW-QOL	0.14	0.21	0.49***	0.36***	0.27*	0.38***	0.77***	0.69***
$P\dot{V}O_2$		0.74***	0.29**	0.01	0.08	0.09	0.07	0.09
$\dot{V}O_2$ at AT			0.32**	0.14	0.20	0.01	0.04	0.18
SAS				0.35**	0.32**	0.30**	0.37***	0.43***
SIP total					0.74***	0.81***	0.31**	0.25*
SIP physical						0.40***	0.12	0.18
SIP psychosocial							0.37***	0.28**
STAI								0.73***

Correlation coefficients and their statistical significance are presented.
Data both before and after 3-month comprehensive cardiac rehabilitation for all 44 patients were included for regression analysis.
*Abbreviations as in Table 2. *p<0.05, **p<0.01, ***p<0.001.*

STAI −10.7%, p<0.05; SDS −9.8%, p<0.05).

Changes in Anxiety and Depression (Fig 3)

When the patients were divided into 2 groups according to the initial STAI score ≥ or <50%, 22 patients (50.0%) with STAI score ≥50% (ie, anxiety state) showed a significant improvement after CCR (58.2±6.1 to 53.0±9.3, p< 0.05), but the remaining 22 patients with initial STAI score <50% (ie, normal) showed no significant change. When the patients were divided into 2 groups according to the initial SDS score ≥ or <50%, 12 patients (27.3%) with SDS score ≥50% (ie, depressive state) showed a significant improvement in SDS score after CCR (58.2±4.4 to 49.7±6.4, p< 0.01), butthe remaining 32 patients with initial SDS score <50% (ie, normal) showed no significant change.

Correlations Between MHW-QOL and Other QOL Scores (Table 4)

The MHW-QOL score significantly correlated with SAS (r=0.49, p<0.001) and SIP total score (r=0.36, p<0.001), indicating that MHW-QOL represents the overall QOL of cardiac patients. Intriguingly, the MHW-QOL score correlated very tightly with the SIP psychosocial disorder score (r=0.38, p<0.001), STAI (r=0.77, p<0.001) and SDS (r=0.69, p<0.001), but less tightly with the SIP physical disorder score (r=0.27, p<0.05) and not significantly with $P\dot{V}O_2$ (r=0.14, NS) or $\dot{V}O_2$ at AT (r=0.21, NS). These findings suggest that in cardiac patients MHW-QOL mainly reflects the psychosocial and mental aspects of QOL rather than physical aspects.

Discussion

The major findings of the present study are that (1) exercise capacity and physical function-related QOL scores (ie, SAS and SIP physical disorder score) significantly improved, whereas psychosocial and mental aspect-related QOL scores (SIP psychosocial disorder score, MHW-QOL, STAI, and SDS) did not change in the whole patient group participating in the 3-month CCR program after AMI, (2) patients with impaired exercise capacity at baseline showed significant improvements in all QOL scores including both physical function-related scores and psychosocial and mental aspect-related scores, whereas patients with preserved exercise capacity showed improvements only in physical function-related QOL scores, (3) patients with anxiety or depression at baseline showed an improvement in each score after CCR, whereas those without anxiety or depression showed no change, and finally, (4) the MHW-QOL score correlated more tightly with psychosocial/mental function-related QOL scores rather than with physical function-related aspects.

Previous Studies

Many previous studies have demonstrated the benefits of CCR for QOL in patients after AMI[1–4,6,7,20–22] but most have used only 1 or 2 QOL instruments and assessed changes in QOL scores after CCR in the whole group. In other words, few studies have investigated which aspect of QOL (physical, psychosocial or mental aspects) is most improved by CCR, which QOL instruments are most sensitive to changes occurring during CCR, and what type of patients obtain the

greatest benefit from CCR after AMI. In fact, Jolliffe et al noted in their meta-analysis that it was not possible to combine the data from studies reporting health-related QOL as an outcome, because 18 different instruments were used in the 11 randomized studies reporting it as an outcome.[25] Shephard et al also noted that there were few direct comparisons between different types of QOL instruments.

One direct comparisons was made by Taylor et al, who utilized 3 generic QOL instruments, including SIP, to assess changes in QOL over time in 88 patients after AMI, and found that all 3 QOL instruments had modest sensitivity.[26] Smith et al[27] compared 4 QOL instruments, including the Medical Outcome Study 36-item Short Form Survey (SF-36),[28] in 22 cardiac patients before and after CCR, and found that only 1 of the SF-36 subscales, vitality, significantly improved over time, from which they concluded that all 4 QOL measures lacked sensitivity to change. In Japan, where most QOL questionnaires invented in Western countries and written in English cannot be directly applied to Japanese patients, comparative assessments of the different QOL instruments during CCR has not been done so far. Yoshida et al studied the MHW-QOL, STAI and SDS in patients with AMI participating in 2-week hospitalized CCR, but did not analyze correlations among the measures.[6] Seki et al also investigated SF-36, STAI and SDS in elderly patients with coronary artery disease participating in phase III CCR, but did not analyze correlations among the measures.[29] Thus, the optimal QOL test instrument or the best method of interpreting the resultant scores there has not been established.

Present Study

In the present study, we compared 5 different QOL instruments in Japanese patients participating in a 3-month CCR program with supervised exercise training and education after AMI. This enabled us to analyze which aspect of QOL improves after CCR and what type of patients gain the greatest improvement in QOL from CCR after AMI. In addition, we were able to determine the nature of the Japan-invented MHW-QOL by assessing the correlations between MHW-QOL and other established QOL scales.

Improvement in QOL After CCR

The present study has shown that $P\dot{V}O_2$, SAS, SIP total score and SIP physical disorder score significantly improved, whereas the SIP psychosocial disorder score, MHW-QOL, STAI, and SDS did not change in the whole patient group after CCR, which indicates that overall the physical function-related QOL scores improved, but the psychosocial and mental aspect-related QOL scores did not. Therefore, not all aspects of QOL (or all types of QOL scores) necessarily improve after CCR in patients with AMI.

Many previous studies have demonstrated an improvement in physical function-related QOL after CCR,[4,20,30–32] but the improvement in mental/psychosocial aspect-related QOL has been inconsistent; some studies have reported a significant improvement,[20,30–33] and others have not.[34–36] For example, Sledge et al[30] and Tyni-Lenne et al[31] reported significant improvements in all areas of QOL (overall, physical, and psychosocial scores) in an 8-week CR program in cardiac patients, whereas Worcester et al[35] and Daumer et al[36] reported no significant difference in the psychosocial and mental aspects of QOL between an exercise training group and a control group. Recently, Izawa et al,[37] using SF-36,[28] reported significant improvements in the physical function-related SF-36 subscales (ie, physical functioning, role-physical, general health) but not in the mental function-related subscales (ie, social functioning, role-emotional, mental health) after CCR in patients with AMI. Thus, whether or not QOL improves after CCR in cardiac patients appears to depend on the aspect of QOL and the type of QOL instrument.

Patient Characteristics Predicting Improved QOL After CCR

In the present study, patients with impaired exercise capacity at baseline showed significant improvements in all QOL scores, including both physical function-related QOL scores and psychosocial and mental aspect-related QOL scores, whereas patients with preserved exercise capacity showed improvements only in physical function-related QOL scores. A potential explanation for this new finding is that there might be a "ceiling effect" (ie, patients with lower initial values have a greater improvement), because the low exercise capacity group in the present study tended to have worse QOL scores at the beginning of CCR (Table 3). In support of this, Lavie et al reported that elderly patients with coronary artery disease had a lower baseline $P\dot{V}O_2$ value, but a greater improvement in QOL score (SF-36), after CCR than younger patients,[38] although Oldridge et al reported that higher exercise tolerance at baseline predicts a greater improvement in the quality of well-being in patients with AMI participating in CCR.[39] The reason for this discrepancy is unclear, and further studies are necessary to address this issue.

The present study also demonstrated that patients with anxiety or depression at baseline showed a significant improvement in each score after CCR, whereas those without showed no change. This finding is in accordance with Oldridge et al[39] who stated that a poor baseline health-related QOL was the predominant predictor of improved generic and specific health-related QOL after CCR. Likewise, Milani et al showed that depressed patients exhibited a greater improvement in psychosocial/mental aspect-related QOL than did normal patients.[40] Again, this finding may well be explained by the ceiling effect. Taken together, the findings suggest that an improvement in QOL after CCR depends not only on the type of QOL instrument but also on the patient characteristics at baseline, and that patients with impaired QOL, anxiety, or depression at baseline should be strongly recommended to participate in CCR with an expectation of greater improvements than patients without these problems.

QOL Instruments for Japanese Cardiac Patients

Although MHW-QOL was originally invented in Japan, no study to date has systematically compared it with other established QOL instruments in patients with AMI participating in CCR. The present study has demonstrated that MHW-QOL reflects overall QOL, as indicated by a significant correlation with SIP total score, but that it mainly represents psychosocial/mental aspect-related QOL rather than physical aspect-related QOL, as indicated by the tight correlations with SIP psychosocial score, STAI and SDS (Table 4).

Recently, SF-36 (Japanese version) has become used more frequently in the field of CCR.[29,37] In fact, a recent review of generic health-related QOL instruments[41] suggests that the SF-36 health survey is the most commonly

used of the generic QOL instruments reviewed.[42] However, some studies have raised a concern that SF-36 may not be sufficiently sensitive to measure the changes in QOL following CCR in cardiac patients.[27,43] Because a perfect QOL instrument for cardiac patients has not been established in Japan, further studies are needed to comparatively assess multiple QOL instruments and to invent a more appropriate QOL instrument for Japanese cardiac patients.

Study Limitations

First, because the present study did not have a control group not participating in CCR, it is unclear whether the improvement in QOL observed is attributable to the favorable effect of CCR or the natural course after AMI. However, the purpose of the present study was to compare different types of QOL instruments rather than to examine the efficacy of CCR on QOL in patients with AMI. To determine whether CCR improves QOL in Japanese patients after AMI, a prospective randomized study will be needed.

Second, the present study did not employ SF-36;[25] however, as mentioned before, it remains unclear whether SF-36 is the most appropriate instrument to assess QOL in Japanese patients participating in CCR after AMI. Further studies are needed to directly compare the usefulness and validity of various QOL instruments, such as MHW-QOL, SIP, and SF-36, in Japanese patients participating in CCR.

Third, the present study assessed changes in QOL in a relatively short-term (ie, 3 months) CCR program. Assessment of the effects of a longer term CCR on QOL in patients with AMI may also be necessary. Finally, because the present study included only a small number of elderly (6 patients (14%) >70 years of age) and female patients (7 (16%) female patients), the present results cannot be directly applied to such specific populations.

Conclusion

In patients with AMI, physical function-related QOL scores improve after 3-month CCR, whereas psychosocial and mental aspect-related QOL scores improve only in those with impaired exercise tolerance or impaired mental function at baseline. Thus, changes in QOL after CCR depend on the type of QOL scales and the patient's baseline status of physical and mental function. In addition, the present study demonstrated for the first time that MHW-QOL mainly reflects psychosocial/mental aspect-related QOL, as well as overall QOL, in Japanese cardiac patients.

Acknowledgment

This work was supported in part by research grants for cardiovascular disease (11C-7, 13C-3 and 15A-2) from the Ministry of Health, Labor and Welfare, Japan.

References

1. Shephard RJ, Franklin B. Changes in the quality of life: A major goal of cardiac rehabilitation. *J Cardiopulm Rehabil* 2001; **21:** 189–200.
2. McGee HM, Hevey D, Horgan JH. Psychosocial outcome assessments for use in cardiac rehabilitation service evaluation: A 10-year systematic review. *Soc Sci Med* 1999; **48:** 1373–1393.
3. Linden W, Stossel C, Maurice J. Psychosocial interventions for patients with coronary artery disease: A meta-analysis. *Arch Intern Med* 1996; **156:** 745–752.
4. Dugmore LD, Tipson RJ, Phillips MH, Flint EJ, Stentiford NH, Bone MF, et al. Changes in cardiorespiratory fitness, psychological well-being, quality of life, and vocational status following a 12 month cardiac exercise rehabilitation programme. *Heart* 1999; **81:** 359–366.
5. Kayaba K, Nagashima K, Saito M, Omae T, Seki A, Arakawa K, et al. The development of quality of life scales for Japanese patients with cardiovascular disease. *J Jpn Assoc Cerebro-Cardiovasc Dis Cont* 1990; **25:** 89–96.
6. Yoshida T, Yoshida K, Yamamoto C. Effects of a two-week, hospitalized phase II cardiac rehabilitation program on physical capacity, lipid profiles and psychological variables in patients with acute myocardial infarction. *Jpn Circ J* 2001; **65:** 87–93.
7. Fujiwara M, Asakuma S, Iwasaki T. Long-term effects of non-supervised home exercise therapy on quality of life in patients with myocardial infarction. *J Cardiol* 2000; **36:** 213–219.
8. Otsuka Y, Takaki H, Okano Y, Satoh T, Aihara N, Matsumoto T, et al. Exercise training without ventricular remodeling in patients with moderate to severe left ventricular dysfunction early after acute myocardial infarction. *Int J Cardiol* 2003; **87:** 237–244.
9. Sakuragi S, Takagi S, Suzuki S, Sakamaki F, Takaki H, Aihara N, et al. Patients with large myocardial infarction gain a greater improvement in exercise capacity after exercise training than those with small to medium infarction. *Clin Cardiol* 2003; **26:** 280–286.
10. Takagi S, Sakuragi S, Baba T, Takaki H, Aihara N, Yasumura Y, et al. Predictors of left ventricular remodeling in patients with acute myocardial infarction participating in cardiac rehabilitation: Brain natriuretic peptide and anterior infarction. *Circ J* 2004; **68:** 214–219.
11. Karvonen M, Kentala K, Mustala O. The effects of training on heart rate: A longitudinal study. *Ann Med Exp Biol Fenn* 1957; **35:** 307–315.
12. Fletcher GF, Balady GJ, Amsterdam EA, Chaitman B, Eckel R, Fleg J, et al. Exercise standards for testing and training: A Statement for Healthcare Professionals From the American Heart Association. *Circulation* 2001; **104:** 1694–1740.
13. Borg G. Perceived exertion as an indicator of somatic stress. *Scand J Rehabil Med* 1970; **2:** 92–98.
14. Uchida I, Takaki H, Kobayashi Y, Okano Y, Satoh T, Matsubara T, et al. O_2 extraction during exercise determines training effect after cardiac rehabilitation in myocardial infarction. *Circ J* 2002; **66:** 891–896.
15. Beaver WL, Wasserman K, Whipp BJ. A new method for detecting anaerobic threshold by gas exchange. *J Appl Physiol* 1986; **60:** 2020–2027.
16. Gibbons RJ, Balady GJ, Beasley JW, Bricker JT, Duvernoy WFC, Froelicher VF, et al. ACC/AHA guidelines for exercise testing: A report of the American College of Cardiology/American Heart Association Task Force on Practice Guidelines (Committee on Exercise Testing). *J Am Coll Cardiol* 1997; **30:** 260–315.
17. Goldman L, Hashimoto B, Cook EF, Loscalzo A. Comparative reproducibility and validity of systems for assessing cardiovascular functional class: Advantages of a new specific activity scale. *Circulation* 1981; **64:** 1227–1234.
18. The EPOCH Study Group. Effects of pimobendan on adverse cardiac events and physical activities in patients with mild to moderate chronic heart failure: The effects of pimobendan on chronic heart failure study (EPOCH study). *Circ J* 2002; **66:** 149–157.
19. Gilson BS, Gilson JS, Bergner M, Bobbit RA, Kressel S, Pollard WE, et al. The sickness impact profile: Development of an outcome measure of health care. *Am J Public Health* 1975; **65:** 1304–1310.
20. Ott CR, Sivarajan EJ, Newton KM, Bruce RA, Gilson BA. A controlled randomized study of early cardiac rehabilitation: The Sickness Impact Profile as an assessment tool. *Heart Lung* 1983; **12:** 162–170.
21. Loose MS, Fernhall B. Differences in quality of life among male and female cardiac rehabilitation participants. *J Cardiopulm Rehabil* 1995; **15:** 225–231.
22. Marchionni N, Fattirolli F, Fumagalli S, Oldridge NB, Del Lungo F, Bonechi F, et al. Determinants of exercise tolerance after acute myocardial infarction in older persons. *J Am Geriatr Soc* 2000; **48:** 146–153.
23. Spielberger CD, Gorsuch R, Lushene R. Manual for state-trait anxiety inventory. Palo Alto, CA: Consulting Psychologists Press, 1970.
24. Zung WW, Durham NC. A self-rating depression scale. *Arch Gen Psychiatry* 1965; **12:** 63–70.
25. Jolliffe JA, Rees K, Taylor RS, Thompson D, Oldridge N, Ebrahim S. Exercise-based rehabilitation for coronary artery disease. *Cochrane Database Syst Rev* 2000; **4:** CD001800.
26. Taylor R, Kirby B, Burdon D, Caves R. The assessment of recovery in patients after myocardial infarction using three generic quality-of-life measures. *J Cardiopulm Rehabil* 1998; **18:** 139–144.
27. Smith HJ, Taylor R, Mitchell A. A comparison of four quality of life instruments in cardiac patients: SF-36, QLI, QLMI, and SEIQoL. *Heart* 2000; **84:** 390–394.

28. Ware JE Jr, Sherbourne CD. The MOS 36-item short-form health survey (SF-36). I: Conceptual framework and item selection. *Med Care* 1992; **30:** 473–483.
29. Seki E, Watanabe Y, Sunayama S, Iwama Y, Shimada K, Kawakami K, et al. Effects of phase III cardiac rehabilitation programs on health-related quality of life in elderly patients with coronary artery disease: Juntendo Cardiac Rehabilitation Program (J-CARP). *Circ J* 2003; **67:** 73–77.
30. Sledge SB, Ragsdale K, Tabb J, Jarmukli N. Comparison of intensive outpatient cardiac rehabilitation to standard outpatient care in veterans: Effects on quality of life. *J Cardiopulm Rehabil* 2000; **20:** 383–388.
31. Tyni-Lenne R, Gordon A, Europe E, Jansson E, Sylven C. Exercise-based rehabilitation improves skeletal muscle capacity, exercise tolerance, and quality of life in both women and men with chronic heart failure. *J Card Fail* 1998; **4:** 9–17.
32. Stahle A, Mattsson E, Ryden L, UNden A, Nordlander R. Improved physical fitness and quality of life following training of elderly patients after acute coronary events: A 1 year follow-up randomized controlled study. *Eur Heart J* 1999; **20:** 1475–1484.
33. Taylor CB, Houston-Miller N, Ahn DK, Haskell W, DeBusk RF. The effects of exercise training programs on psychosocial improvement in uncomplicated postmyocardial infarction patients. *J Psychosom Res* 1986; **30:** 581–587.
34. Oldridge N, Guyatt G, Jones N, Crowe J, Singer J, Feeny D, et al. Effects on quality of life with comprehensive rehabilitation after acute myocardial infarction. *Am J Cardiol* 1991; **67:** 1084–1089.
35. Worcester MC, Hare DL, Oliver RG, Reid MA, Goble AJ. Early programmes of high and low intensity exercise and quality of life after acute myocardial infarction. *BMJ* 1993; **307:** 1244–1247.
36. Daumer R, Miller P. Effects of cardiac rehabilitation on psychosocial functioning and life satisfaction on coronary artery disease clients. *Rehabil Nurs* 1992; **17:** 69–72.
37. Izawa K, Hirano Y, Yamada S, Oka K, Omiya K, Iijima S. Improvement in physiological outcomes and health-related quality of life following cardiac rehabilitation in patients with acute myocardial infarction. *Circ J* 2004; **68:** 315–320.
38. Lavie CJ, Milani RV. Disparate effects of improving aerobic exercise capacity and quality of life after cardiac rehabilitation in young and elderly coronary patients. *J Cardiopulm Rehabil* 2000; **20:** 235–240.
39. Oldridge N, Gottlieb M, Guyatt G, Jones N, Streiner D, Feeny D. Predictors of health-related quality of life with cardiac rehabilitation after acute myocardial infarction. *J Cardiopulm Rehabil* 1998; **18:** 95–103.
40. Milani RV, Lavie CJ, Cassidy MM. Effects of cardiac rehabilitation and exercise training programs on depression in patients after major coronary events. *Am Heart J* 1996; **132:** 726–732.
41. Coons SF, Rao S, Keininger DL, Hays RD. A comparative review of generic quality of life instruments. *Pharmacoeconomics* 2000; **7:** 13–35.
42. Oldridge N. Assessing health-related quality of life: Is it important when evaluating the effectiveness of cardiac rehabilitation? *J Cardiopulm Rehabil* 2003; **23:** 26–28.
43. Hawkes AL, Nowak M, Speare R. Short Form-36 Health Survey as an evaluation tool for cardiac rehabilitation programs: Is it appropriate? *J Cardiopulm Rehabil* 2003; **23:** 22–25.

Circ J 2005; **69:** 1315–1319

Angiotensin-Converting Enzyme Genotype is Not Associated With Exercise Capacity or the Training Effect of Cardiac Rehabilitation in Patients After Acute Myocardial Infarction

Yoshitaka Iwanaga, MD; Isao Nishi, MD; Koh Ono, MD; Shuichi Takagi, MD; Yoshiaki Tsutsumi, MD; Masanori Ozaki, MD; Teruo Noguchi, MD; Hiroshi Takaki, MD; Naoharu Iwai, MD; Hiroshi Nonogi, MD; Yoichi Goto, MD

Background The relationship of the genotype for the angiotensin-converting enzyme (ACE) with exercise capacity or training effects has been studied in athletes or healthy persons, but recently the ACE DD genotype was reported to be associated with decreased exercise capacity in patients with congestive heart failure. Therefore, in the present study the association between the ACE genotype and exercise capacity was investigated in patients with acute myocardial infarction (AMI) participating in cardiac rehabilitation (CR) for 3 months.

Methods and Results The study population comprised 168 patients stratified as II (n=75), ID (n=67), and DD (n=26) according to ACE genotype. Baseline left ventricular ejection fraction (LVEF) was similar among the genotype groups. In all patients, exercise capacity (peak work rate (PWR) and peak oxygen uptake ($P\dot{V}O_2$)) significantly increased after CR. However, no differences were observed in PWR and $P\dot{V}O_2$ among the genotype groups at baseline or after CR. The results were similar even when analyzed in 60 patients with left ventricular (LV) dysfunction (LVEF <45%).

Conclusion The present study suggests that there is no association between ACE I/D polymorphism and exercise capacity in patients after AMI, even with LV dysfunction. Furthermore, ACE genotype may have no influence on the effects of CR after AMI. (*Circ J* 2005; **69:** 1315–1319)

Key Words: ACE genotype; Cardiac rehabilitation; Left ventricular dysfunction; Myocardial infarction

Exercise-based cardiac rehabilitation (CR) improves functional capacity and reduces mortality in patients with acute myocardial infarction (AMI)[1–3] Although the exact mechanisms by which exercise reduces mortality are unclear, one of the definite effects is improving exercise tolerance[4,5] Exercise tolerance itself is a multifactorial phenotype influenced by several genetic and environmental factors and the training benefits may be attributed predominantly to adaptations in the peripheral circulation and skeletal muscles rather than to adaptations in cardiac performance[6] However, the precise mechanism is not fully understood.

Over the past decade, the insertion/deletion (I/D) polymorphism of a 287-bpAlu element in intron 16 of the angiotensin-converting enzyme (ACE) gene has been extensively investigated in a spectrum of cardiovascular phenotypes, because of its correlation with serum ACE activity[7] Many of the previous studies have shown a positive association between the DD genotype and an increased risk of MI, and recent reports suggested a potential pharmacogenetic interaction between the ACE genotype and therapy with β-blockers in chronic heart failure (CHF) patients[8] However, results in hypertension, left ventricular (LV) hypertrophy, cardiomyopathy and restenosis after percutaneous transluminal coronary angioplasty remain quite controversial.

Several studies have shown that the ACE I allele is associated with enhanced physical performance. An increased frequency of the ACE I allele has been reported in army recruits, rowers, and high altitude mountaineers[9,10] The ACE I allele has been associated with higher peak oxygen consumption ($P\dot{V}O_2$) levels in postmenopausal women[11] Moreover, a recent study has demonstrated an association of the ACE DD genotype with decreased exercise tolerance in 57 patients with CHF[12] However, the association between ACE genotype and exercise capacity or the effect of exercise training in patients after AMI with or without LV dysfunction remains unknown. Accordingly, in the current study, we examined exercise capacity in relation to ACE polymorphism in patients with AMI participating in CR for 3 months.

Methods

Study Population

One hundred sixty-eight consecutive patients who were admitted to the National Cardiovascular Center with a diagnosis of AMI and participated in the 3-month CR program with exercise training between January 2001 and September 2002 were recruited. The CR program started approximately 2 weeks after the onset of AMI and continued for 3 months. Patients exercised for 60 min 4–5 times a

(Received June 27, 2005; revised manuscript received August 9, 2005; accepted August 30, 2005)
National Cardiovascular Center, Suita, Japan
Mailing address: Yoichi Goto, MD, Division of Cardiology, National Cardiovascular Center, 5-7-1 Fujishirodai, Suita 565-8565, Japan. E-mail: ygoto@hsp.ncvc.go.jp